

ABSTRACT

**BIOMECHANICAL ANALYSIS OF
ASYMMETRIC AND DYNAMIC LIFTING TASK**

by
Xiaopeng Jiang

Lifting tasks is one of the leading causes of occupational lower back disorders (LBD). Aimed at deriving internal forces of human musculoskeletal system during lifting, biomechanical models are utilized to address this problem. This thesis provides an in-depth literature review of such modeling, and the results of experiments used to address LBD issues.

An isometric pulling experiment was conducted to study the correlation between electromyography (EMG) and muscle forces predicted by AnyBody Modeling System™ with increasing hand loads, and infinite order polynomial (min/max) optimization criterion predicted percentage of maximum muscle forces 98% correlated with normalized EMG. In a separate study, motion data during lifting of 13.6kg (30lb) weight at 0°, 30° and 60° asymmetry was collected by the OptiTrack™ six-camera motion capture system to drive the AnyBody™ model dynamically. Erector spinae was the most activated muscle during lifting. When the lifting origin became more asymmetric toward right, the right external oblique was more activated, and complementarily the right Internal oblique was less activated. Because oblique muscles with larger moment arms can support an external moment more efficiently, and the subject squatted more as the lifting origin became more asymmetric, L5/S1 joint forces decreased.

This study contributes to the design and evaluation of lifting tasks to minimize the cost of LBD.

**BIOMECHANICAL ANALYSIS OF
ASYMMETRIC AND DYNAMIC LIFTING TASK**

**by
Xiaopeng Jiang**

**A Thesis
Submitted to the Faculty of
New Jersey Institute of Technology
in Partial Fulfillment of the Requirements for the Degree of
Master of Science in Occupational Safety and Health Engineering**

Department of Mechanical and Industrial Engineering

May 2011

Copyright © 2011 by Xiaopeng Jiang
ALL RIGHTS RESERVED.

APPROVAL PAGE

**BIOMECHANICAL ANALYSIS OF
ASYMMETRIC AND DYNAMIC LIFTING TASK**

Xiaopeng Jiang

| | |
|--|------|
| Dr. Arijit K. Sengupta, Thesis Advisor Associate Professor of Mechanical and Industrial Engineering, NJIT | Date |
|--|------|

| | |
|--|------|
| Dr. Athanassios Bladikas, Committee Member Associate Professor of Mechanical and Industrial Engineering, NJIT | Date |
|--|------|

| | |
|--|------|
| Dr. George Olsen, Committee Member Adjunct Professor of Mechanical and Industrial Engineering, NJIT | Date |
|--|------|

BIOGRAPHICAL SKETCH

Author: Xiaopeng Jiang

Degree: Master of Science

Date: May 2011

Date of Birth: March 10th, 1987

Place of Birth: Zhengzhou, P. R. China

Undergraduate and Graduate Education:

- Master of Science in Occupational Safety & Health Engineering,
New Jersey Institute of Technology, Newark, NJ, 2011
- Bachelor of Engineering in Safety Engineering,
Northeastern University, Shenyang, P. R. China, 2009

Major: Occupational Safety & Health Engineering

To Those Whom I Love
And Those Who Love Me

ACKNOWLEDGMENT

I would like to begin by expressing my deepest appreciation to Dr. Arijit K. Sengupta, who not only served as my research supervisor, providing valuable and countless resources, insight, and intuition, but also constantly gave me support, encouragement, and reassurance. I would like to thank NYNJ Education and Research Center, National Institute of Occupational Safety and Health (NIOSH), whose financial support helped to make this thesis possible. Special thanks are given to Dr. Athanassios Bladikas and Dr. George Olsen for actively participating in my committee.

I want to thank Dr. Richard Foulds more for letting me use the motion capture system in his laboratory. I also want to express gratitude to my friends who participated in this study: Gul, Hua and Ziqian.

TABLE OF CONTENTS

| Chapter | Page |
|---|------|
| 1 INTRUDUCTION..... | 1 |
| 1.1 Background..... | 1 |
| 1.2 Objectives..... | 6 |
| 2 LITERATURE REVIEW..... | 8 |
| 2.1 Anatomical Modeling..... | 8 |
| 2.1.1 Single Muscle Equivalent Model..... | 9 |
| 2.1.2 Ten-Muscle Model..... | 11 |
| 2.1.3 Anatomically Detailed Model..... | 12 |
| 2.1.4 Geometric Torso Model..... | 13 |
| 2.1.5 Discussion..... | 15 |
| 2.2 Kinetic Modeling..... | 18 |
| 2.2.1 Statically Determinate Model..... | 18 |
| 2.2.2 Optimization Criterion Based Model..... | 19 |
| 2.2.3 EMG-assisted Model..... | 21 |
| 2.2.4 Regression Model..... | 25 |
| 2.2.5 Comparison Study..... | 26 |
| 2.2.6 Discussion..... | 28 |

TABLE OF CONTENTS (Continued)

| Chapter | Page |
|--|------|
| 2.3 AnyBody Modeling System™..... | 30 |
| 2.3.1 Lumbar Spinal Model..... | 31 |
| 2.3.2 Muscle Recruitment Optimization Criterion..... | 32 |
| 3 MUSCLE ACTIVITY & PREDICTED MUSCLE FORCE..... | 36 |
| 3.1 Methods and Materials..... | 36 |
| 3.2 Results..... | 39 |
| 4 ASYMMETRIC EFFECT IN DYNAMIC LIFTING TASK | 45 |
| 4.1 Methods and Materials | 45 |
| 4.2 Results..... | 47 |
| 5 CONCLUSION AND FUTUTRE WORK..... | 52 |
| REFERENCES..... | 54 |

LIST OF TABLES

| Table | Page |
|---|------|
| 2.1 Summary of Characteristics of the Models..... | 16 |
| 4.1 Maximum Muscle Forces in Newton during Each Task..... | 48 |
| 4.2 Maximum Joint Forces in Newton during Each Task..... | 49 |

LIST OF FIGURES

| Figure | Page |
|--|------|
| 2.1 Schematic diagram of single muscle equivalent model..... | 10 |
| 2.2 Schematic diagram of the 10-muscle model..... | 11 |
| 2.3 Vector representation of the trunk used in the EMG-assisted model..... | 12 |
| 2.4 Muscle geometry illustrated for a 50 th -percentile male..... | 14 |
| 2.5 Representation of global and local musculatures..... | 15 |
| 2.6 AnyBody™ full body human musculoskeletal model..... | 31 |
| 2.7 Comparison of L4/L5 joint compression force predicted by AnyBody™ with Wilke et al.'s in-vivo intervertebral disc pressure measurement..... | 35 |
| 3.1 Static pulling task on a wooden platform..... | 37 |
| 3.2 Percentage of maximum longissimus EMG RMS and predicted muscle force | 40 |
| 3.3 Percentage of maximum longissimus EMG RMS and predicted muscle force | 40 |
| 3.4 Predicted L4/L5 joint compression forces with gradually increasing hand load of the three criteria in flexed trunk straight arm posture..... | 43 |
| 3.5 Predicted L4/L5 joint shear forces with gradually increasing hand load of the three criteria in flexed trunk straight arm posture..... | 43 |
| 3.6 Predicted psoas major force with gradually increasing hand load of the three criteria in flexed trunk straight arm posture..... | 44 |
| 4.1 Asymmetric lifting task configuration..... | 46 |
| 4.2 First frames of 0°, 30° and 60° asymmetric lifting initialized in inverse dynamic study by AnyBody™ model..... | 47 |

CHAPTER 1

INTRODUCTION

1.1 Background

Lower back disorder (LBD) related to occupational manual material handling (MMH) is still not fully understood. According to the U.S. Centers for Disease Control and Prevention (CDC) [1], MMH may expose workers to physical conditions, e.g., force, awkward postures, and repetitive motions, that can lead to injuries to the back, shoulders, hands, wrists, or other parts of the body, wasted energy, and wasted time. Injuries may include damage to muscles, tendons, ligaments, nerves, and blood vessels. Injuries of this type are known as musculoskeletal disorders (MSDs). According to the U.S. Bureau of Labor Statistics [2], MSDs accounted for 28 percent of all injuries, and the back was injured in nearly half of the MSD cases and required median of 7 days to recuperate. Out of all the MMH tasks, lifting has been the main contributors to the lower back injuries, accounting for 49-60 percent of lower back incidents [3].

Low back pain (LBP) is the most common clinical, social, economic, and public health problem affecting the population indiscriminately across the world among all chronic pain conditions. It is estimated that 28% of the U.S. industrial population will experience disabling low back pain at some time and 8% of the entire working population will be disabled in any given year, contributing to 40% of all lost work days. In fact, workers' compensation programs in the 50 states and the District of Columbia and federal programs in the United States combined paid \$56 billion in medical and cash benefits in 2004, an increase of 2.3% over 2003 payments. In addition, occupational

diseases represented only 8% of the claims and 29% of the cost [4]. The employers lose useful manpower and may have to employ and pay replacement workers.

It is generally accepted that occupational LBP is a manifestation of overloading back extensor muscles and spinal tissues during lifting tasks. Although many basic properties of the human musculoskeletal system are measurable, internal forces in living tissues can rarely be measured directly during lifting task performance. Biomechanical modeling has been utilized to investigate lifting task characteristics so that the task demands can be kept within a limit and the strength capacity of internal muscles and joints are not exceeded. During lifting activity, considerable forces can be generated on the back extensor muscles and the vertebral discs, including compression and shear forces. This approach focuses on determining forces and moments acting on the body during lifting tasks and their effects on various body segments, muscles and joints. To determine internal tissue forces and moments more accurately, progressively more detailed anatomical models of the lower back have been introduced in modeling. Current anatomical models of the lower back cannot only consider all major muscle groups relevant in lifting activity, but also the muscle model can differentiate among the individual muscle fascicles of a muscle group [5, 6] with consideration of muscle wrapping against bony structures [5-8]. In biomechanics, the muscle and joint forces are determined from Newtonian mechanics. However, due to the presence of redundant muscle groups that may be active during such activities, the statics problem essentially becomes a statically indeterminate problem. The statically indeterminate problems are over defined, and as a result, Newtonian mechanics alone cannot predict the muscle forces. Two types of kinetic models have been developed to solve such statically

indeterminate problems: (i) optimization criterion based and (ii) electromyography (EMG) assisted. Optimization criterion based models assume that muscles are recruited in such a way that a criterion function is minimized to reduce a biological cost, such as joint compression force [9, 10] and muscle fatigue functions [11-13]. This type of optimization approach is based on the assumption that the human central nervous system (CNS) has the ability to recruit muscles in a way that will provide maximum protection against internal injury. EMG assisted models utilize measured myoelectric activity to represent muscle recruitment patterns.

Several EMG assisted biomechanical models have been developed with varying degree of sophistications [7, 14]. Essentially, these models partitioned the total extensor moment during lifting into different muscle groups based on EMG signals collected from surface electromyography. In surface electromyography, electrodes are affixed on the skin surface over a muscle of interest and the electrical potential picked up by the electrode provides a measure of spatial and temporal summation of electrical activities of the underlying muscle fibers. It has been well documented that the muscle tension correlates well with the electrode potential provided the muscle contraction is isometric, that is, muscle fiber lengths remain unchanged during force production. However, during dynamic situation, when muscle fibers generate force as well as change their lengths, sliding action of muscle fibers underneath the fixed surface electrodes, also generates electrode potential [15]. Unless the dynamic part of the electrode potentials are separated from the gross electrode potential, the EMG would not accurately estimate force generation by the muscle fibers, and as a result partitioning of the extensor muscle tensions would not be accurate. None of the EMG based models has described how the

dynamic part of the EMG was separated from the static EMG, and hence the model outcomes are questionable.

Apart from the computational complexity due to redundant musculature, asymmetric effects during dynamic lifting tasks add significant complexity to such models. Asymmetry occurs when an external load is handled in a non-sagittal plane. Three dimensional (3D) equilibriums of forces and moments are needed to be considered in such cases. Dynamic lifting tasks involve the change in velocity (acceleration/deceleration) during movement of body parts. Inertial forces develop on all moving masses during such a motion, which affects the internal tissue loading. To take into account the inertial forces, the change in velocity of each body part needs to be tracked by some form of motion capture system, which provides time varying 3D coordinate data of moving body segments. A great variety of workstation layouts in workplaces are associated with asymmetric and dynamic lifting. Thus, to obtain the most accurate estimation of internal tissue loading, the induction of asymmetric and dynamic characteristics is crucial to the investigation.

Trunk kinematics characteristics, including range of motion, peak velocity, average velocity, and peak acceleration, increase with an increase in task asymmetry [16-19], which increases the resultant trunk moments. During asymmetric lifts, the support of the external load is shifted from the central erector spinae muscles to smaller, less capable oblique muscles [20]. Marras and Davis [18] found that the right latissimus dorsi, right erector spinae, right internal oblique, and right external oblique muscles all exhibited increased activity when lifting from origins located to the left of the sagittal plane. For spine joint forces, they reported that compression and lateral shear forces

increased as the lift origin became more asymmetric, whereas anterior-posterior shear forces decreased [18].

The AnyBody Modeling System™ [21] developed at Aalborg University is a general-purpose musculoskeletal modeling and simulation program. AnyBody™ can provide detailed results such as individual muscle forces, joint forces and moments, metabolism, elastic energy in tendons, and antagonistic muscle actions. AnyBody™ is also scalable in terms of segment mass, length and muscle strength to fit to any population or individual from anthropometric data [22]. The essential features of this computer program can be summarized as follows:

1. AnyBody™ models are open and editable, i.e. maximum muscle force, segment mass, posture, etc data are editable.
2. Complex geometries of muscles, bones, ligaments, tendons, etc. and their spatial arrangement and interactions have been and can be readily modeled within AnyBody Modeling System™ [23]. Body models with unprecedented detail can be handled efficiently [22].
3. Data can be imported from motion capture (mocap) systems to drive AnyBody™ models dynamically [22]. Drivers can also be defined without captured data to drive the models [24].
4. To solve muscle redundancy problem, the AnyBody Modeling System™ offers a choice of several optimization-based muscle-recruitment criteria in inverse-dynamics study [24].

The AnyBody™ provides by far the most detailed human torso musculoskeletal model. Unlike any other model, it simulates more closely individual muscles, in terms of their fascicle attachments. Muscle models are more realistic, in the sense that it can take into account the muscle length and velocity of contraction to estimate the maximum force generation capacity. Thus far, the torso model of AnyBody™ has been utilized effectively to validate internal muscle and joint forces [23, 25-27], but none of the studies investigated the effect of asymmetric and dynamic aspects of lifting.

Since the AnyBody Modeling System TM is a general purpose modeling tool, it comes with a choice of mathematical optimization functions to solve the muscle redundancy problem. It is expected that the user will select the appropriate function that produces most accurate results for the particular modeling being undertaken.

The mathematical implementation of the optimization function is of the following form:

$$\min \sum \left(\frac{f_i}{N_i} \right)^p \quad (1.0)$$

Where, f_i = force generated in muscle i ,
 N_i = maximum force capacity of muscle i , and
 p = polynomial power.

The term (f_i/N_i) is essentially the percent of capacity of a muscle being used and hence is related to muscle fatigue factor. AnyBodyTM provides a selection of the power of the polynomial $p = 1$ to 5 and infinite (min/max). Previous researchers have indicated that infinite polynomial power is suitable for the torso muscle model [6]; however this has not been explicitly validated by an experimental study.

1.2 Objectives

Based on the above discussion, the objectives of this thesis are defined as following:

- Conduct a literature review on biomechanical models of lifting tasks;
- Conduct a laboratory experiment to investigate the relationship between normalized EMG with the predicted percentage of maximum muscle forces, and the effect of different optimization criterion functions in AnyBodyTM on predicting lumbar joint forces;

- Utilize a motion capture system in an asymmetric dynamic lifting task, and use the AnyBody™ software with an appropriate optimization criterion to investigate internal tissue loading.

CHAPTER 2

LITERATURE REVIEW

This chapter presents a literature review of human torso biomechanical modeling, for the purpose of estimating internal muscle and lumbar joint forces during the performance of lifting tasks. The first two sections describe the evolution in anatomical modeling, kinetic modeling, and the third section describes the AnyBody™ system of modeling that integrates many of the recent development in biomechanical modeling.

2.1 Anatomical Modeling

The first step toward the biomechanical modeling related to lifting tasks is to develop an anatomical model of the human musculoskeletal system. One basic assumption in biomechanical modeling is that the body is made up of rigid body segments joined at known, simple articulations. This is more valid for the arms and legs, than the trunk, which is a semi-flexible arrangement of vertebral bodies, intervertebral discs and cartilaginous endplates located between the vertebral bodies and discs [28]. The anatomy of the spine is described by dividing up the spine into three major sections: the cervical, the thoracic, and the lumbar spine. Below the lumbar spine is a bony structure, called the sacrum (S1), which is attached to the pelvic bone. Each section is made up of individual bony structure called vertebrae. There are 7 cervical vertebrae (C1-C7), 12 thoracic vertebrae (T1-T12), and 5 lumbar vertebrae (L1-L5). In many biomechanical models, the lower lumbar L4/L5 or lumbosacral L5/S1 disc is chosen for particular attention. This was based on statistics, which showed that between 85% and 95% of all disc herniations occur with relatively equal frequencies at the L4/L5 and L5/S1 levels. Since the L5/S1 disc is the lower most vertebral disc, it carries the greatest amount of

compressive load. It was also reported that these discs were most often shown in X-rays of the vertebral column to have the greatest amount of degeneration when compared to other discs [29]. Anatomical models of varied details have been developed to estimate joint loading in the lower lumbar joints. The following sections describe these anatomical models of the human torso with increasing order of complexity.

2.1.1 Single Muscle Equivalent Model

This torso model assumes that the major back extensor muscle group erector spinae (ES) is responsible for developing the extensor moment during sagittal lifting. Figure 2.1 shows a schematic diagram of single muscle equivalent model. The torso is represented by two segments, a pelvic-sacral segment and a lumbar-thoracic segment, connected at the lumbosacral joint L5/S1 [28]. The lumbar extensor musculature ES is modeled 5cm posterior to the disc center of L5/S1, which is considered the center of rotation for the purpose of computation of moment [28]. In the vertical erect posture of the torso, the L5/S1 joint was assumed to be at 19.5% of the distance between the hip and shoulder. The amount of forward pelvic rotation relative to lumbar rotation was determined by the amount of trunk flexion.

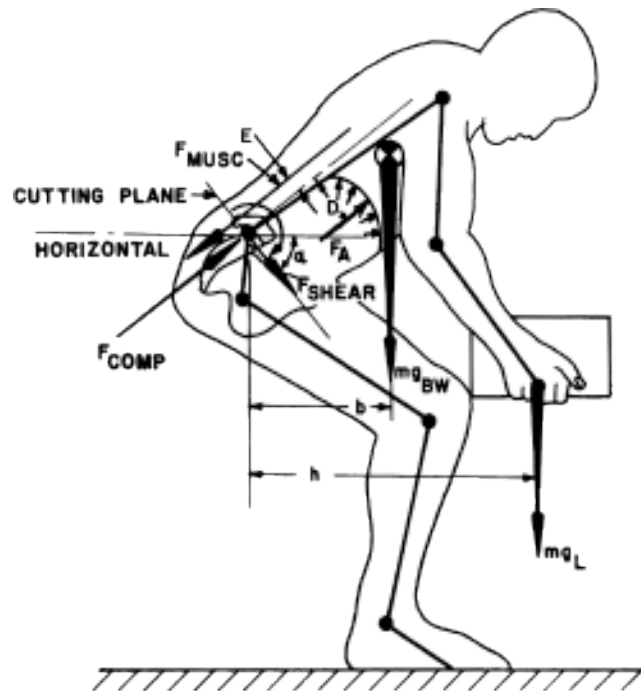


Figure 2.1 Schematic diagram of single muscle equivalent model [30].

The model parameters, such as the muscle moment arm, location of the center of L5/S1 and the ratio of pelvis to lumbar rotation were derived from adult population anthropometry and computer tomography (CT) scan and X-ray images of the trunk. The single muscle model is considered to be adequate for purely sagittal lifting, when the internal and external forces are coplanar representing a two dimensional (2D) lifting situation. Due to the presence of only one unknown muscle force in such 2D analysis, the internal joint and muscle forces can be determined from the equilibrium of forces and moments, and hence, the model is statically determinate. However, when the trunk moves away from the mid-sagittal plane, other major muscle groups become active. Since this model had no provision for the muscles that are responsible for the axial rotation of the torso, this model is not amenable for analyzing asymmetric lifting.

2.1.2 Ten-Muscle Model

Schultz et al. [31] first considered additional muscles in a three dimensional (3D) analysis of forces. The model divided the torso muscles at the lumbar region into five pairs (left and right): rectus abdominus (R), external oblique (E), internal oblique (I), erector spinae (S), and latissimus dorsi (L) (Figure 2.2). This model includes ten unknown muscle forces, compression, lateral shear and anterior-posterior (A-P) shear forces of L5/S1 joint, and is thus statically indeterminate. Muscle recruitment optimization algorithms are introduced based on the assumption that muscles are recruited to minimize certain functions of muscle force, which will be discussed later in more detail under the kinetic modeling section. The 3D Static Strength Prediction Program™ (3DSSPP™) software [32] developed by University of Michigan is based on this anatomical model.

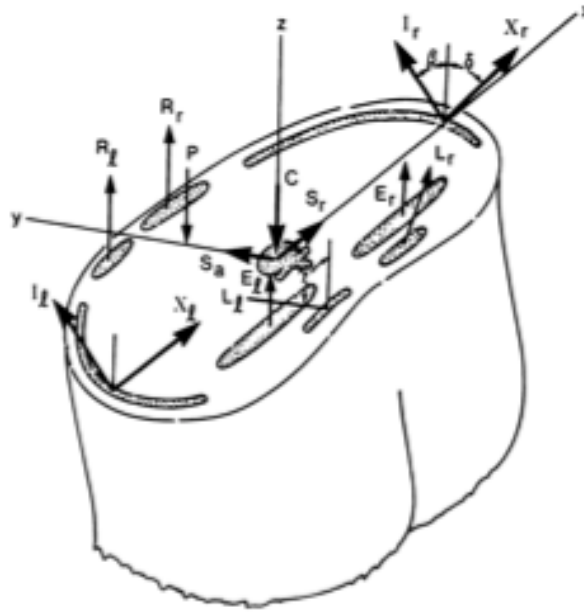


Figure 2.2 Schematic diagram of the 10-muscle model [31].

Marras and Granata [14] developed a similar lumbar torso musculature model (Figure 2.3). The muscles included in this model were the same as the model described above: rectus abdominus (RcA), external oblique (ExO), internal oblique (InO), erector

spinae (ErS), and latissimus dorsi (Lat). Muscle origins were assigned a three-dimensional location relative to the spinal axis, co-planar with the iliac crest. Muscle insertions are located co-planar with the 12th rib. This model not only accounted for postural variations in muscle length-tension predictions, but also included a velocity-tension modifier to provide better estimates of dynamic muscle tensions from EMG estimates, which will be discussed further under the kinetic modeling section.

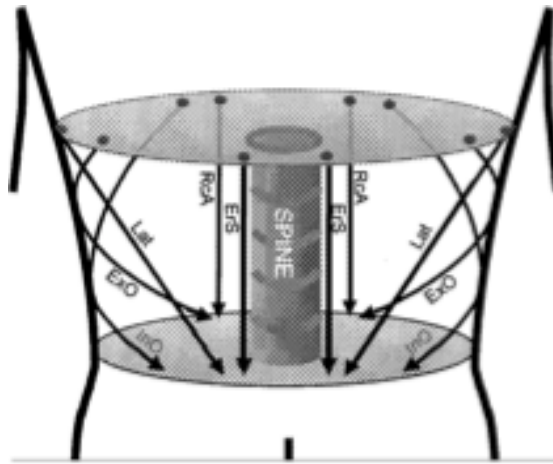


Figure 2.3 Vector representation of the trunk used in the EMG-assisted model [14].

2.1.3 Anatomically Detailed Model

Aimed at creating a model as anatomically accurate as possible, the model built by McGill and Norman [7] incorporated 48 muscles, and 7 ligaments. The 3D skeleton comprised of a pelvis, rib cage, and five lumbar vertebrae modeled from archived radiologic records and corresponding to a 50th-percentile adult man. The flexion of the five vertebrae (R_i) was predicted according to the linear-decline relationship (α_i) from the total lumbar flexion (F_t): $R_i = \alpha_i(\text{L1 and L2: } 13.2\%, \text{ L3: } 21\%, \text{ L4: } 29\%, \text{ L5: } 23.6\%)* F_t$. Disc deformations were modeled as a third order polynomial estimated from the joint compression force, because disc behavior could not be modeled the same way as that of linear elastic bodies. Ligaments were connected to the appropriate skeletal points and

exerted force. The algorithm for the individual muscle geometric representation began by assuming a straight line between origin and insertion. This length was then modified by an approximation of the individual muscles by circular arcs. Hence, muscles with an S-shaped orientation, such as the laminas of sacrospinalis, were modeled as two circular arcs arranged with opposing convexity. Muscle tendon length was subtracted from the total to gain an accurate measure of the muscle-active component length.

2.1.4 Geometric Torso Model

With the advent of improved anatomical dissection and imaging techniques, it is becoming possible to understand the complicated effects of varied muscle and ligament geometries. CT and ultrasound scans and other methods are producing accurate spatial representations necessary to define the precise lines of action of torso muscles and their associated skeletal components [29]. Nussbaum and Chaffin [8] developed a torso model (Figure 2.4) with the lines of action of major muscles depicted relative to a cutting plane at the L3/L4 discs, including erector spinae, rectus abdominis, internal oblique, external oblique, latissimus dorsi, transversus abdominis, psoas, and quadratus lumborum. Muscles are treated as point-wise connections from origin to insertion. By combining this type of geometric model with muscle force representations that include both active and passive tension relationships, it has become possible to begin to understand how various torso postures and asymmetric loading combinations cause specific low back tissue stresses [29].

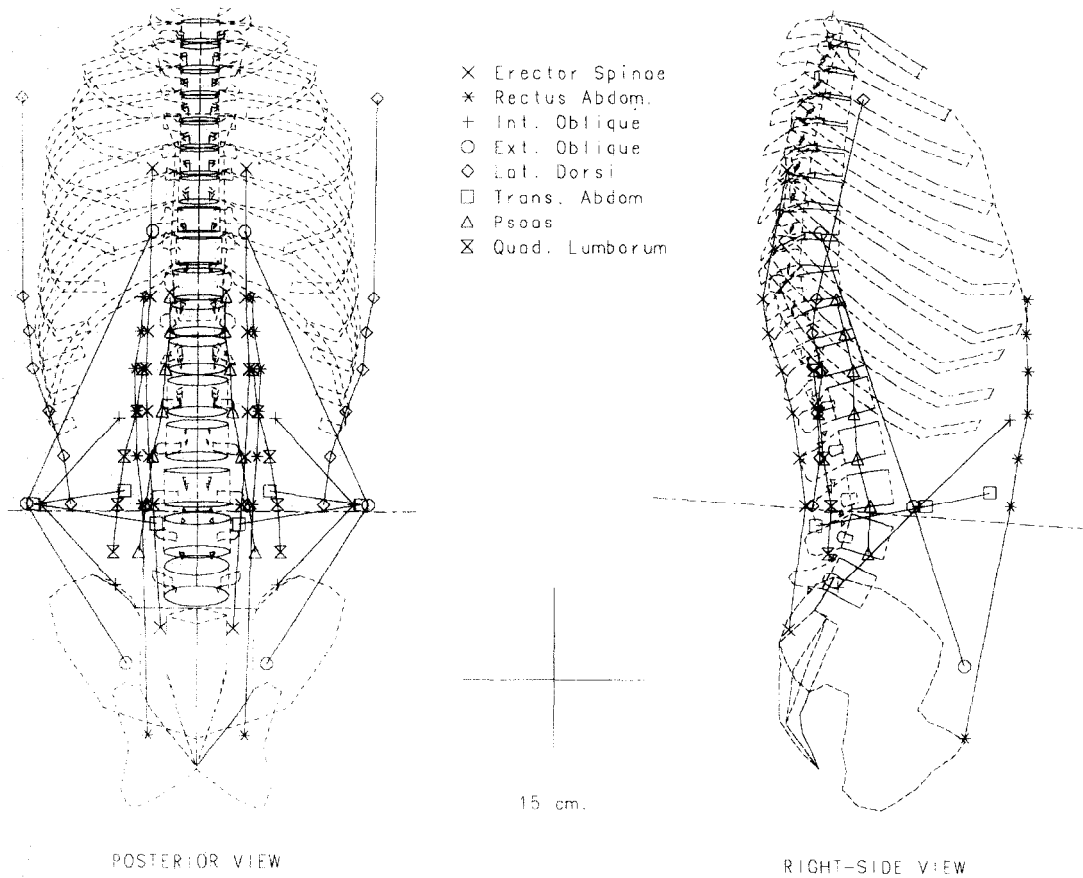


Figure 2.4 Muscle geometry illustrated for a 50th-percentile male. An imaginary cutting plane that bisects the L3/L4 motion segment is also shown [8].

Recently, Arjmand et al. [5, 11, 33-37] used a similar anatomical model (Figure 2.5), which included iliocostalis lumborum pars lumborum (ICpl), iliocostalis lumborum pars thoracic (ICpt), iliopsoas (IP), longissimus thoracis pars lumborum (LGpl), longissimus thoracis pars thoracic (LGpt), multifidus (MF), quadratus lumborum (QL), internal oblique (IO), external oblique (EO), and rectus abdominus (RA), combining with finite element (FE) analysis and optimization algorithms to evaluate muscle recruitment, internal loads and stability margin. Their study also mentioned how vertebral disks were modeled so that every disc was flexible. They used a sagittally symmetric T1–S1 beam-rigid body model comprising six deformable beams to represent T12–S1 discs and seven rigid elements to represent T1–T12 as a single body and lumbosacral vertebrae (L1–S1).

The beams modeled the overall nonlinear stiffness of T12–S1 motion segments, i.e., vertebrae, disc, facets and ligaments, at different directions and levels. The nonlinear load–displacement response under single and combined axial/shear forces and sagittal/lateral/axial moments along with the flexion versus extension differences were represented in this model based on numerical and measured results of previous single- and multi-motion segment studies.

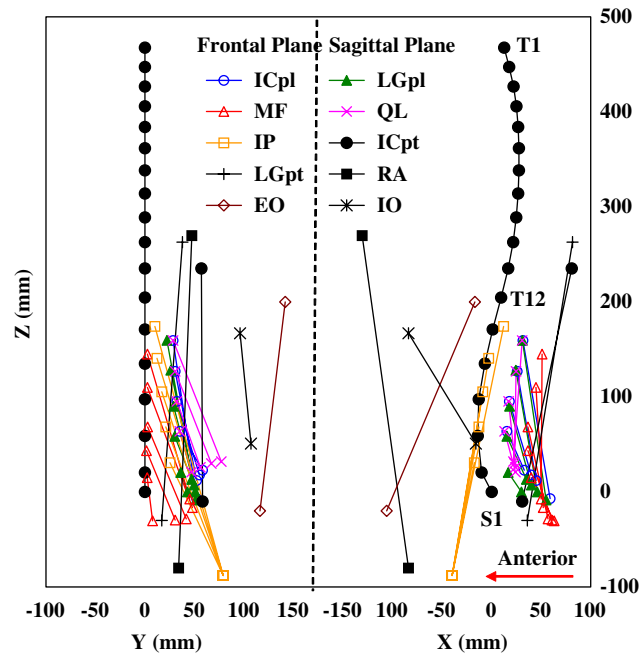


Figure 2.5 Representation of global and local musculatures in the sagittal (X) and frontal (Y) planes used in the FE model. Only fascicles at one side have been shown in frontal plane [5].

2.1.5 Discussion

The characteristics of the anatomical models mentioned above are summarized in Table 2.1. Anatomical modeling should be as realistic and detailed as possible, which is also the trend in the development process. From a single muscle anatomical model [28], more recent models included 10 muscle groups [5, 8] to represent torso musculature.

Table 2.1 Summary of Characteristics of the Models

| Anatomical models | Number of trunk muscles groups | Flexible trunk plane | Trunk muscle force vector representation | Erector spinae divided into divisions? | Muscles divided into fascicles? | Number of ligaments |
|-------------------------------------|--------------------------------|----------------------|--|--|---------------------------------|---------------------|
| Single muscle equivalent model [28] | 1 | L5/S1 | Straight and parallel to torso | No | No | 0 |
| Ten-muscle model [31] | 2*5 | L4/L5 | Straight and parallel to torso | No | No | 0 |
| Ten-muscle model [14] | 2*5 | 12th rib, L5/S1 | Straight but individually aligned | No | No | 0 |
| Anatomically detailed model [7] | 2*10 | L1-L5 | Individually aligned and contain arcs or S-shaped | Yes | No | 7 |
| Geometric torso model [8] | 2*8 | T1-L5 | Individually aligned and passes over attachment points | No | No | 0 |
| Geometric torso model [5] | 2*10 | T1-L5 | Individually aligned and passes over attachment points | Yes | Yes | 0 |

To accomplish a realistic muscle force vector representation, the spine cannot just be considered flexible at a single level, because the curvature of the spine influences the position of vertebral disks, which in turn influences muscle force direction if a realistic muscle attachment is used. It has also been demonstrated that consideration of equilibrium at a single spine level yields results in violation of equilibrium at the remaining levels, especially so in more demanding tasks [34]. Marras and Davis [14] first considered two flexible spinal planes at the 12th rib, L5/S1 to determine the muscle force vectors. Subsequent models introduced more flexible spine segments, including joints between T1 to L5.

Trunk muscles included in the biomechanical models should realistically represent the torso musculature. Traditionally, muscles have been modeled as exerting force along straight lines. The first two models in Table 2.1 considered muscle force vectors acting along straight lines parallel to the trunk axis. However, many muscles within the trunk act around pulley systems of bone, other muscle bulk, and pressurized viscera, which alter both length and force vector properties [7]. According to Arjmand et al. [33], muscle forces and spinal compression at all levels decrease as trunk extensor muscles took curved paths. In contrast, the shear force at lower levels increased. Despite smaller muscle forces, wrapping of muscles improved the spinal stability. Arjmand et al. [33] also studied the moment arm importance on extensor moments of individual muscle groups. Allowing for a 10% reduction in these lever arms during flexion increased muscle forces and compression forces at all levels. Their results indicated that consideration of muscles with curved paths and realistic lever arms are important in biomechanical analysis of lifting tasks. Muscle modeling to implement curved paths was introduced by McGill and Norman [7] and subsequently Nussbaum and Chaffin [8], Arjmand et al. [5, 11, 33-37] incorporated this aspect by means of intermediate attachment points within individual muscle groups.

The muscles considered should not be simplified and grouped as synergic sets. According to Bogduk [38], the analysis must consider large muscle groups such as erector spinae as a continuum of independent fibers because a single equivalent force cannot represent their action. It should be even better when each muscle fascicle is modeled. McGill and Norman [7] first modeled erector spinae into divisions, and Arjmand et al. [5, 11, 33-37] further incorporated fascicles of each muscle group.

Spinal ligaments are elastic bodies that attach two vertebral bodies in a spinal joint, and their passive elasticity might provide some extensor moments during spinal motion. McGill and Norman [7] incorporated seven different ligaments in the torso model but contribution to tissue loading was found to be insignificant compared to that from extensor muscles. Other models presume no significant contribution to extensor moment production from ligaments.

2.2 Kinetic Modeling

After building the anatomical model, Newton's equilibrium of forces and moments can be established. The external forces and moments generated by gravity are equated to the internal force and moments, to determine the unknown muscle and joint forces. As has been discussed in the previous section, for models that incorporate more than one muscle group to model an asymmetric lifting condition, redundancy of muscles prevents direct solution from Newtonian mechanics and the solution of internal forces becomes statically indeterminate. The following sections describe different approaches in kinetic modeling to solve such statically indeterminate problems.

Furthermore, when a body is in motion, acceleration-deceleration of masses may introduce inertial forces. As a human motion is executed, complex inertial forces are created by changes in the velocity and direction of the motion of the body segments. Inertial forces are modeled at the segment centroids according to Newton's second law of motion.

2.2.1 Statically Determinate Model

Historically, single muscle equivalent models have been criticized on the fact that during demanding lifts they predict disc compression force and erector spinae muscle force greater than the tolerance, while the subject is apparently not injured [39]. Intra-abdominal pressure (IAP) has been hypothesized to exert a force over the inferior surface of the diaphragm creating an extensor moment on the lumbar spine. Freivalds et al. [28] considered IAP to offset the excessive extensor moment produced only by the muscles. The CG of the combined head and trunk is assumed to be located on a straight line between the shoulder and hip joint during trunk flexion. Erector spinae muscles as a group with a moment arm fixed at 5 cm provided the extension moment along with the extensor moment produced by IAP (Figure 2.1). In their force and moment equilibria, the only two unknowns to be solved are the erector spinae muscle force and spine compressive force at the L5/S1 level. The abdominal force and moment were derived from a regression equation. The L5/S1 compression force then can be further split into compression and shear forces. As has been discussed before, this model is only applicable for a 2D sagittal lifting situation.

2.2.2 Optimization Criterion Based Model

As stated earlier, many more muscles are activated and responsible for the joint force during lifting, especially for asymmetric lifting. Redundancy of muscles during such lifting conditions makes the number of unknown forces exceed the number of equilibrium equations of force and moment and the problem becomes statically indeterminate. Muscle recruitment optimization algorithms are introduced based on the assumptions that muscles are recruited to minimize certain physiological functions.

The spine compression force is a factor that has strong correlation with occupational LBP. In a linear programming (LP)-based model [9], the minimization of the spine compressive forces was used as an objective function. Constraint functions were developed from the equilibrium of three-dimensional forces and moments on the activity of ten trunk muscles along with the IAP force equated to the external forces and moments acting on the upper body. However, the muscle contraction intensities should also not exceed a reasonable level. Based on the joint requirement of minimizing both joint compressive force as well as muscle contraction intensities, Bean et al. [10] suggested a double LP optimization procedure. First, an upper bound on muscle intensity is found by minimizing the maximum muscle intensity such that the moment equilibrium conditions are satisfied; and second, the muscle forces satisfying the moment conditions and muscle intensity bounds, which minimize the muscular contribution to spinal compression force, are determined. Chaffin et al. [29] developed 3DSSPP™ based on a double LP, which can calculate L4/L5 compression force and shear force, muscle force of left and right erector spinae, rectus abdominis, left and right obliquus internus and externus, left and right latissimus dorsi. The muscles mentioned above were grouped as synergic sets acting parallel to the trunk axis without consideration of a complex lumbar anatomy (no trunk muscle wrapping) [37]. The 3D back compression optimization is computed at the L4/L5 lumbar from ten torso muscles at the L4/L5 level by double LP [40].

Rasmussen [12] compared two known optimization criterion types: the polynomial criterion and the soft saturation criterion. The comparison is performed on a planar three-muscle elbow model performing a dumbbell curl. It is concluded that the

min/max criterion (infinite power polynomial criterion) possesses a number of attractive physiological as well as algorithmic advantages. Their algorithm aimed at minimizing $G(\mathbf{f}^{(M)})$, which were represented by the following equation for the polynomial and soft saturation criterion respectively (equation 2.1). The polynomial criterion is actually a family of muscle recruitment optimization algorithms by defining p and N_i differently.

$$\begin{aligned} G(f^{(M)}) &= \sum_{j=1}^{n^{(M)}} \left(\frac{f_i^{(M)}}{N_i} \right)^p \\ G(f^{(M)}) &= - \sum_{i=1}^{n^{(M)}} \sqrt{1 - \left(\frac{f_i^{(M)}}{N_i} \right)^2} \end{aligned} \quad (2.1)$$

2.2.3 EMG-assisted Model

EMG is electrical signals generated by the action potentials, which can be sensed using skin or needle electrodes placed near the muscle. Normalized EMG is associated with muscle force. However, the relationship is most consistent and linear when muscle action is isometric, muscle length is consistent between trials, and muscles increase force by increasing their motor neuron firing rate, not by recruiting additional motor units. Instead of optimization algorithms, EMG can also be collected to represent muscle activation, which can be used as the criterion of muscle recruitment. This kind of model is able to explain how the trunk muscles work collectively (co-contraction) to support the external load, and account for the variability in muscle recruitment.

In the model of McGill and Norman [7], the crude estimation of joint moments was first derived from film coordinate data, body mass and forces in the hands. In order

to partition the resultant moment into restorative components provided by the disc, ligaments, and musculature, the disc and ligamentous moments were determined first because their strain is flexion dependent, and the remaining moment was allocated to the musculature. The musculature was driven from surface EMG collected from six sites, which were normalized to a statically determined maximum voluntary contraction (MVC). Each muscle was described mathematically in terms of ability to generate force with consideration of muscle length, cross-sectional area, velocity, passive elasticity, and a common gain factor. A common gain to all muscles was calculated, using a least mean square (LMS) regression over the duration of each ramp trial, to obtain the best fit between the EMG predicted and measured moments in all three axes. This gain was implemented to compensate for systematic errors in the initial assessment of muscle force producing potential and their cross-sectional areas. The modulated muscle forces were finally applied to the skeleton to calculate joint force. They found that estimations of the L4/L5 disc compression and shear were 16.2% and 42.5% lower than those calculated from a simple 5cm erector tissue moment arm length. They concluded that there was no need to invoke IAP or other contentious compression-reducing mechanisms. Actually, IAP is depicted as a by-product of antagonistic co-contraction of the torsos muscles during the act of slow lifting, and is ignored in the more recent reduced models [29]. Muscle activity, particularly that of the sacrospinalis, dominated the generation of the restorative moment. Ligaments played a very minor role in the lifts study.

Cholewicki et al. [41] incorporated the optimization method's advantage of forcing equilibrium in the reaction moments into the EMG method to develop an EMG assisted optimization (EMGAO) approach. This approach consisted of a correction to the

EMG assisted estimates of muscle forces by multiplying gains (g_i) to satisfy all three-moment equilibrium constraints simultaneously. The objective function was to ensure the least possible gain adjustment to the individual muscle forces estimated from EMG, which are mathematically formulated as equation 2.2. However, the differences between the joint compression results given by the EMG and EMGAO methods were minimal.

$$\sum_{i=1}^n M_i (1 - g_i)^2 = \min, \quad M_i = \sqrt{M_{x_i}^2 + M_{y_i}^2 + M_{z_i}^2} \quad (2.2)$$

Marras et al. [14] followed McGill's modeling concepts, but their model depended more on empirical results. Geometrically, this model assumed that one could represent the trunk mechanically via a description of the transverse cutting plane passed through the lumbar spine. It only included muscles that can be documented via direct EMG measurement so that muscle activity assumptions could be avoided.

The tensile force generated by each muscle, j , was described by the product of normalized EMG, muscle cross-sectional area, a gain factor representing muscle force per unit area, and modulation factors describing EMG and force behavior as a function of the length $f(\text{Length}_j)$, and velocity, $f(\text{Vel}_j)$ of muscle j (equation 2.3).

$$Force_j = Gain \frac{EMG_j(t)}{EMG_{j\max}} Area_j f(Vel_j) f(Length_j) \quad (2.3)$$

Pre-assuming the functions of the length and velocity were 3rd and 2nd order polynomials respectively (equation 2.4), the coefficients were determined by minimizing

the average variation in predicted gain as a function of length/Velocity. The length/velocity modulation factor employed the instantaneous length of muscle, j , determined from the anthropometry coefficients and kinematic input.

$$\begin{aligned} f(\text{Length}_j) &= -3.2 + 10.2 \text{Length}_j - 10.4 \text{Length}_j^2 + 4.6 \text{Length}_j^3 \\ f(\text{Vel}_j) &= 1.2 - 0.9 \text{Vel}_j + 0.72 \text{Vel}_j^2 \end{aligned} \quad (2.4)$$

Voluntarily applied external kinetics, including gravitational moments and acceleration effects on trunk mass were dynamically measured by a force plate and pelvic stabilization system. Translation of force plate mechanics was performed to compute 3D moments about the lumbosacral spine. The pelvic stabilization system permits free dynamic motion above the pelvis or of the whole body. This was accomplished by mathematically correcting for the position of the pelvis relative to the force plate. Gain was computed by comparing muscle-generated trunk moments with measured applied moments. Spinal loadings (compression, right-lateral shear, and anterior shear forces) were calculated from the vector sum of validated muscle forces. Muscle generated moments about the spinal axis were predicted from the sum vector products combining dynamic tensile forces of each muscle, j , and respective moment arms.

Input data required by the model include time-domain EMG of erector spinae, latissimus dorsi, internal oblique, external oblique and rectus abdominus, exertion kinetics, and kinematics. Maximum exertion EMG levels and subject anthropometry were also employed to calibrate and format the dynamic data suitable for use in the model mechanics. The cross-sectional area of each muscle was computed from

regression equations based on the subject's trunk depth and breadth. The equipment include a force plate, a lumbar motion goniometer, and an EMG measuring system.

2.2.4 Regression Model

To simplify the calculation process and to avoid the need of complex data collection, several regression models were built from the results predicted by the existing complex models.

Based on results predicted from a detailed 90 muscle model over a variety of 3-D tasks by EMGAO, the three low-back moments and corresponding spine compression load from the time histories of all subject-trials were used as variables to obtain polynomial equations [42]. While second, third, fourth, and fifth order polynomials were attempted, the third order was chosen as the best compromise between obtaining a realistic fit of the data and minimizing local non-symmetric inflections that are biologically inexplicable, and occur with higher order polynomials. The value of R^2 was 0.936, which indicated that the regression results were very close to the original model.

Similarly, Arjmand [37] established predictive equations that relate responses of a complex detailed trunk finite element biomechanical model to its input variables during sagittal symmetric static lifting activities. Four input variables (thorax flexion angle, lumbar/pelvis ratio, load magnitude, and load position) and four model responses (L4–L5 and L5–S1 disc compression and anterior–posterior shear forces) were considered. Quadratic predictive equations for the spinal loads at the L4–S1 disc mid-heights were obtained by regression analysis with adequate goodness-of-fit ($R^2 > 98\%$). Results indicated that intra-discal pressure values at the L4/L5 disc estimated based on the

predictive equations are in close agreement with available in vivo data [43] measured under similar loadings and postures.

2.2.5 Comparison Study

A series of data sets for validation of models were presented by Wilke et al. [43], including directly measured intradiscal pressure (IDP) and anthropometric data. Most of the models available compared their results with this in-vivo measured data, although the in-vivo data was only measured for some standard static postures. Many comparison studies were also conducted to check the model performance.

Chung et al. [13] evaluated three optimization models (minimize maximum muscle intensity: $\text{MIN_I}_{\text{MAX}}$, minimize sum of magnitudes of the muscle forces raised to power 3: MIN_F^3 , and minimize sum of the muscle intensities raised to power 3: MIN_I^3) under various asymmetric lifting conditions. Muscle intensity is defined as the muscle force divided by the cross-sectional area of the muscle. $\text{MIN_I}_{\text{MAX}}$ exhibits the best prediction capability when comparing it with EMG signals of left erector spinae, left latissimus dorsi and left external oblique muscles among the three optimization models.

Kee and Chung [44] compared three representative methods of predicting the compressive forces on the lumbosacral disc: LP-based model, double LP-based model, and EMG-assisted model. The EMG-assisted model was shown to reflect well all three factors (vertical and lateral distances, and weight of load) considered here, whereas the compressive forces from the two LP-based models were only significantly affected by weight of load.

Fischer et al. [45] examined the impact of different joint models (single muscle equivalent), an electromyography-based third order polynomial, a modified version of the

polynomial and a hybrid approach) to determine cumulative spine compression. Findings demonstrated considerable differences between modeling approaches, which suggested that caution should be taken when selecting a muscle model to determine cumulative spine compressive loading.

Arjmand et al. [11, 35, 36] did several comparison studies on different optimization criteria and different models. First, they [11] investigated the effect of eight different optimization functions ($\sum \text{stress}^3$, $\sum \text{stress}^2$, $\sum \text{force}^2$, $\sum \text{stress}$, $\sum \text{force}$, $\sum \text{axial compression}$, double-linear and muscle fatigue) on trunk muscle forces and spinal loads. Four criteria ($\sum \text{stress}^3$, $\sum \text{stress}^2$, fatigue and double-linear) predicted muscle activities that qualitatively matched measured EMG data, but the fatigue and double-linear criteria were inadequate in predicting greater forces in larger muscles with no consideration for their moment arms. Overall, one single optimization function of $\sum \text{stress}^3$ or $\sum \text{stress}^2$ rather than a multi-criteria function was found sufficient and adequate in yielding plausible results comparable with measured EMG activities and disc pressure.

Second, a comparison of forces and spinal loads estimated by a single-joint EMGAO model and a multi-joint optimization based (minimizing $\sum \text{stress}^3$) finite element model of the spine under different static lifting activities in upright standing posture was completed [35]. They found that external moments, compression forces at the L4–S1 joints and the sum of all trunk muscle forces were somewhat similar, but both models recruited muscles in a markedly different way, which in turn led to significantly different shear force estimates.

Third, they further investigated the performance of two models under symmetric (symmetric trunk flexion from neutral upright to maximum forward flexion) and asymmetric (holding a load at various heights in the right hand) activities [36]. They found that shear and compression forces were generally higher in the optimization-based model, which also predicted greater activities in extensor muscles as compared to the EMGAO model.

2.2.6 Discussion

Statically determinate models oversimplified lifting activity both anatomically and kinetically. Some researchers also questioned the IAP mechanism of the models. The compression cost of the abdominal wall muscular activity required to produce the intra-abdominal pressure has been neglected in the calculation [7]. Even in heavy lifts, the EMG activity of the abdominal musculature required to generate IAP is relatively low, and the correlation of IAP, measured intra-rectally or intra-gastrically, with EMG in isometric holds is also low [39].

Optimization criterion based models can incorporate as many muscles in detail as needed to represent reality, while EMG-assisted models can only include a limited number of muscle sites that can be measured by surface EMG. Another advantage of an optimization criterion based model approach is the precision and continuity of the results with the valid algorithms. The Variability of measured EMG is comparatively large, and EMG measures also suffer from noise and artifacts. As a result, the number of subjects and trials required in an optimization-based study is less than that needed by an EMG-assisted model, making the former more desirable for industry. To get valid results from an optimization algorithm, muscles in the model can be defined in the maximum detail

possible. However, in most of the current models, there are far fewer muscles included than those active during an actual lifting experience. Another weakness of current optimization models is that they are poor at predicting patterns of co-contractions of antagonistic muscles [42]. Even with a sophisticated muscle recruitment optimization criterion, under dynamic conditions, muscle co-contraction, which greatly increases the predicted spinal compression forces over those produced when lifts are made in asymmetric sagittal-plane, is not well-explained [14].

Aimed at addressing the muscle co-contraction problem, an EMG assisted model uses surface EMG to represent muscle recruitment. Besides the disadvantage of larger variability, this kind of model also requires the use of a multi-channel EMG and direct measurement of spine kinematics, which precludes them from being used in the workplace. According to Marras [46] himself, if muscle force is of interest, postural changes should be minimized since muscle length and velocity have a dramatic effect upon muscle force and EMG relationship. However, the EMG-assisted model was used to investigate dynamic lifting, and the EMG was normalized by dividing RMS EMG during dynamic lifting by RMS EMG during static maximum exertion. This is problematic because the numerator EMG not only represented force generation but also incorporated muscle movement under the skin.

Lifting tasks in the workplace are dynamic and vary greatly from trial to trial. If the EMG assisted model is used, standard deviations of the values of interest will be high, which requires many more experimental trials to get valid results than the optimization criterion based models. Theoretically, the EMG should not be measured in dynamic movement to represent force generation, because of the unknown relationship between

EMG and muscle force generation. Therefore, optimization criterion based models are preferred to investigate internal loading during lifting task performance.

2.3 AnyBody Modeling System™

The AnyBody Modeling System™ is essentially an object-oriented programming platform. With the AnyBody Managed Model Repository™ (AMMR), a collection of unique models ready for use has been provided, which can be used to model the human musculoskeletal system in detail readily. The AMMR contains a collection of detailed scalable template body models performing a variety of different activities of daily living. In this model library, different parts of the body are structured, model scaling is determined, draw setting is defined, and a tool box facilitating motion capture, kinematic analysis and kinetic analysis are programmed. A graphical representation of the full body human musculoskeletal model in the AnyBody Modeling System™ is shown in Figure 2.6 to illustrate the details of the model.



Figure 2.6 AnyBody™ full body human musculoskeletal model.

For static studies, body parts, postures and loads can be defined in the scripts, and inverse dynamic studies can be run based a selected optimization criteria. For dynamic studies, either pre-defined drivers as a funtion of time for certain body parts' positions and angles, or a c3d motion capture file can be used to drive the models. The dynamic effects, in terms of inertial forces, are incorporated in inverse dynamic studies to compute internal muscle and joint forces.

2.3.1 Lumbar Spinal Model

For lifting tasks, the most important anatomical modeling part is the lumbar spine. Hansen et al. [47] did a delicate review on a lumbar spinal model, and the AnyBody™ model has incorporated those details [6] based on previous research. The spine model

comprises seven rigid segments: the pelvis, the five lumbar vertebrae and a lumped thoracic part. The musculature provided in the AnyBody™ model represents the real human anatomy most closely comparing with other existing models. The multifidus muscle is divided into nineteen fascicles on each side in three layers. The four divisions of the erector spinae (longissimus thoracis pars lumborum, iliocostalis lumborum pars lumborum, longissimus thoracis pars thoracis and iliocostalis lumborum pars thoracis) are divided into a total of twenty-nine fascicles on each side. The psoas major is divided into eleven fascicles. The quadratus lumborum is represented by five fascicles. Three abdominal muscles are included in the model: rectus abdominus, obliquus externus, and obliquus internus. The rectus abdominus is modeled as one fascicle between the thorax and pelvis via points on the artificial rectus sheath. The obliquus externus and internus are divided into six fascicles each. Fascicles are modeled using straight-line elements for the short fascicles and line elements with via-points for the longer fascicles. Ligaments, the force–length relationship and the force–velocity relationship of individual muscle fascicles are not included in the model, because of lack of reliable information. The maximal force (strength) of each fascicle is predicted from a strength scaling factor, physiological cross sectional area (PCSA) and unit spine muscle tension.

Two other important aspects of lumbar spinal modeling are spine curvature and IAP. For spine curvature, it uses a pre-defined rhythm [48] which links motion between each vertebra together with pelvis/thorax motion. IAP is modeled as constant volume. When squeezed from the side by the transversus muscles, it extends the spine by pushing on the rib thorax and the pelvic floor. From the mathematical point of view, this lets the abdominal muscles function as spine extensors, and they become part of the whole

recruitment process [49]. Anatomically, the AnyBody™ model is more detailed and realistic than the models mentioned before, which makes it a promising tool to investigate LBD in lifting.

2.3.2 Muscle Recruitment Optimization Criterion

The AnyBody Modeling System™ provides users a family of polynomial criteria, with the order of polynomial being 1st to 5th and infinite. As has been explain in the introduction section, the objective function is $\min \sum (f_i/N_i)^p$ in which p is the order of the polynomial, f_i is individual muscle force, and N_i is some choice of normalization factors. Actually, the strength of each muscle is used as N_i . Because the strength of each fascicle around the lumbar spine is modeled from strength scaling factor times unit spine muscle tension, and times physiological cross sectional area (PCSA), the family of criterion for lumbar spine muscles is actually polynomials of muscle intensity (stress) divided by a common gain, which is identical with the criterion used by Chung et al. [13] and Arjmand et al. [11].

Mathematically, the trend of all these algorithms indicated by the objective function is that all terms in the polynomial become equal, based on the Cauchy–Bunyakovsky–Schwarz inequality. f_i s are becoming closer in value with increasing order, because f_i/N_i s are smaller than 1, and $(f_i/N_i)^p$ s are becoming closer in value with increasing order. Physiologically, increasing the power of the criteria makes the muscles to work together better and allow the organism to carry larger loads without overloading any individual muscle. In other words, polynomial criteria of increasing order produce increased degrees of synergism between the muscles. Maximum synergism would be the case where all muscles capable of a positive contribution to balancing the external load

work together in such a way that the maximum relative load of any muscle in the system is as small as possible. This would physiologically be a minimum fatigue criterion because fatigue is likely to happen first in the muscle with the maximum relative load, and it makes physiological sense that the body might work that way. It would mean that the body would minimize muscle fatigue, and precisely this criterion might determine survival of the fittest in an environment where organisms are competing with each other for limited resources [24]. When the polynomial power is increasing towards infinity, then the muscle recruitment criterion would approach a min/max formulation, that is to minimize the maximum intensity of all muscle. This also makes this algorithm computationally feasible.

For joint forces, the AnyBody™ research group checked the results of the infinite order optimization with the in-vivo intervertebral disc pressure measured by Wilke et al. [50]. By setting both to 100% for standing, Figure 2.7 shows that the results of both were close, and lifting a box with a weight of 19.8kg generated joint compression forces two to five times as much as the standing posture.

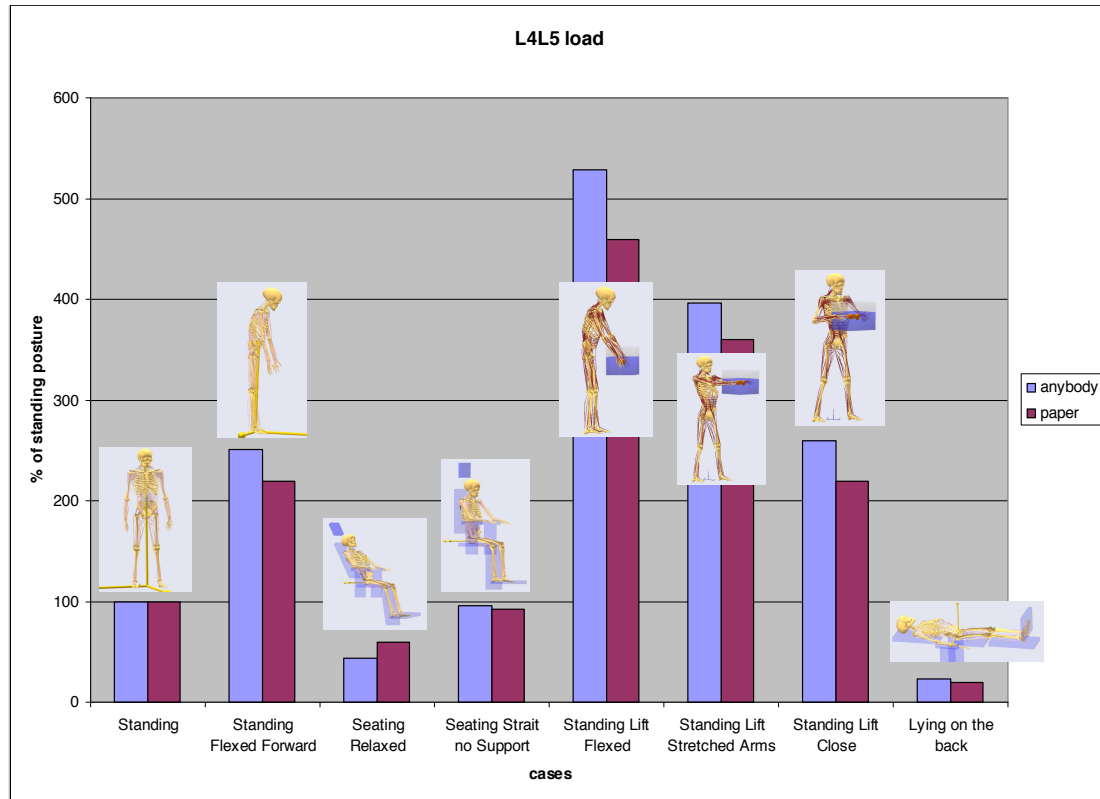


Figure 2.7 Comparison of L4/L5 joint compression force predicted by AnyBody™ with Wilke et al.'s in-vivo intervertebral disc pressure measurement.

From the above analysis, the infinite order polynomial optimization criterion was found to be suitable for static lift analysis. Based on previous comparison studies, Chung et al. [13] found MIN_I_{MAX} , that is, min/max muscle intensity criterion, was best in static lifting comparing with EMG pattern, while Arjmand et al. [11] suggested to use $\sum stress^3$, essentially a 3rd order polynomial function, in predicting joint forces.

However, thus far, the order of polynomial in the optimization criteria has not been investigated for predicted muscle force and normalized EMG relationship with increasing hand load. In addition, the AnyBody™ software's capability of processing motion capture files to include dynamic effect during asymmetric lift has also not been investigated.

CHAPTER 3

MUSCLE ACTIVITY & PREDICTED MUSCLE FORCE

This section describes the laboratory experiment that was carried out to investigate (i) the relationship between measured normalized EMG and the predicted percentage of maximum muscle forces, and (ii) the effect of different optimization criterion functions in the AnyBody Modeling System™ on predicting lumbar joint forces. Since the surface EMG is affected by muscle fiber movement, static lifting tasks were simulated at different hand loads. The simulated lifting tasks were performed in the sagittal plane. In sagittal lifting, erector spinae muscle is the principal extensor [51]. In the AnyBody Modeling System™, this major muscle is modeled by four groups of fascicles, and longissimus and iliocostalis fascicle groups are situated at the lumbar region and are more posterior than the other two fascicles. These two fascicles also have different extensor moment arms defined in the AnyBody Modeling System™. Since these two fascicles can be measured separately by surface EMG, they were selected for EMG measurement in this study. The experimental details and results follow.

3.1 Methods and Materials

One healthy male college student, with height of 178cm, and weight of 70.8kg, without any history of LBD during the past six months performed static sagittal pulling tasks. The tasks involved pulling with hand loads of 76N, 96N, 116N, 136N, and 156N in three selected postures as shown in Figure 3.1. The three postures were straight trunk with arm flexed, flexed trunk with arm straight and flexed trunk with arm flexed respectively, which represented commonly adopted lifting postures. A pulling bar was linked with an adjustable chain and steel rope through a fixed pulley, and was connected to a

horizontally placed load cell fixed by eyebolts (Figure 3.1b). The pulling forces were measured by the load cell; muscle activities of longissimus and iliocostalis were measured by surface EMG electrodes; and pelvis/thorax and hip flexion angles were measured by electrogoniometers. The longissimus and iliocostalis muscle groups are chosen, since the sagittal lifting task is expected to produce significant muscle activities from these two muscle groups.

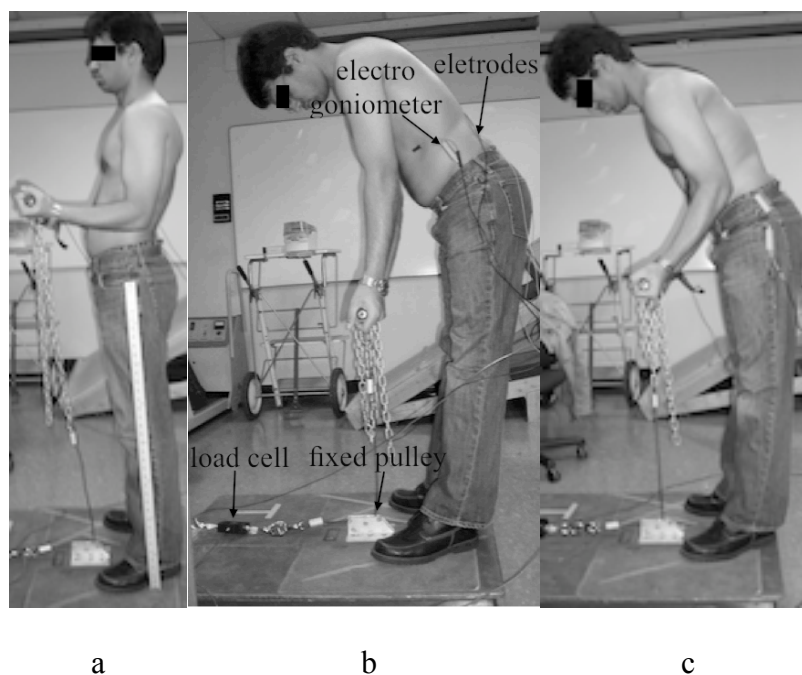


Figure 3.1 Static pulling task on a wooden platform: a. straight trunk with arm flexed, b. flexed trunk with arm straight and c. flexed trunk with arm flexed.

Before the experiment, the participant was informed about the purpose and procedure of the experiment, and his height and weight was recorded. Electrolytic gel was then applied and the electrodes were adhered to the skin with double-faced adhesive tape on cleaned skin surface of the right longissimus and iliocostalis muscle group. For the longissimus muscle group, the electrodes were centered 3 cm lateral to the midline at

the first lumbar vertebra. For the iliocostalis muscle group the electrode was centered at 6 cm lateral to the midline at the third lumbar vertebra [35].

Each foot was placed on the platform at a 30° angle from the sagittal plane. Two electrogoniometers were attached on the lumbar and hip (Figure 3.1b) to measure the pelvis/thorax and hip flexion angles respectively. The rest of the body segment angles were obtained from sagittally taken photos.

EMG electrodes, electrogoniometers and a load cell were connected and synchronized through a DataLINK Base Unit (Biometrics Ltd.) to a desktop PC. After connection, the participant was asked to relax, and all the readings were initialized to zero. EMG data was recorded and analyzed by the DataLINK PC software Version 2.00 (Biometrics Ltd.) with a sampling rate of 1000 data/second and sensitivity of 300mV, while angles and hand loads were recorded and analyzed by the same software with a sampling rate of 200 data/second.

To allow normalization of EMG levels, maximum voluntary contractions (MVCs) of longissimus and iliocostalis were performed three times for 6 seconds for per trial through exertions with the participant lying prone with the lower body supported on a table and the upper body hanging [52]. During the experiment, the participant was asked to increase the hand load 20N per trial from 60N to 140N without changing his posture. The load cell output was visible to the participant on the computer screen, and he was asked to maintain each desired load level for about six seconds. The participant was positioned on the platform such that the direction of the pull was vertically downward. After trials in one posture, the participant was encouraged to rest for 3 minutes. The

weights of the handle bar and the chain, 0.879kg and 0.739kg, respectively, were added to the load cell reading to obtain the hand load.

3.2 Results

After the experiment, the RMS of EMG was computed for each exertion by the DataLINK software using the Triangle/Bartlett moving window of 10 mS for 4 seconds out of the 6 seconds sustaining time, corresponding to the averaged loads read from the load cell. The normalized EMG was calculated as the RMS EMG of the pulling tasks divided by the RMS of the MVC tasks.

To determine the muscle activities predicted by the AnyBody Modeling System™, the “StandingModel” in the AMMRV1.3.1 was modified so that hand forces in “LeftArmDrivers.any” and “RightArmDrivers.any” were defined to increase from 76N to 156N (load cell readings plus the weight of bar and chain) by a 20N increment. Body segment angles from electrogoniometers and sagittal photos were inputted to “Mannequin.any”, and subsequently the inverse dynamic studies defined in “StandingModel.Main.any” were run using the infinite order polynomial optimization criterion. This criterion was found to be more suitable for ergonomic investigations by the AnyBody™ research group [24]. The percentage of maximum muscle forces on the longissimus and iliocostalis were further calculated, and compared with the normalized EMG as shown in Figure 3.2 and Figure 3.3.

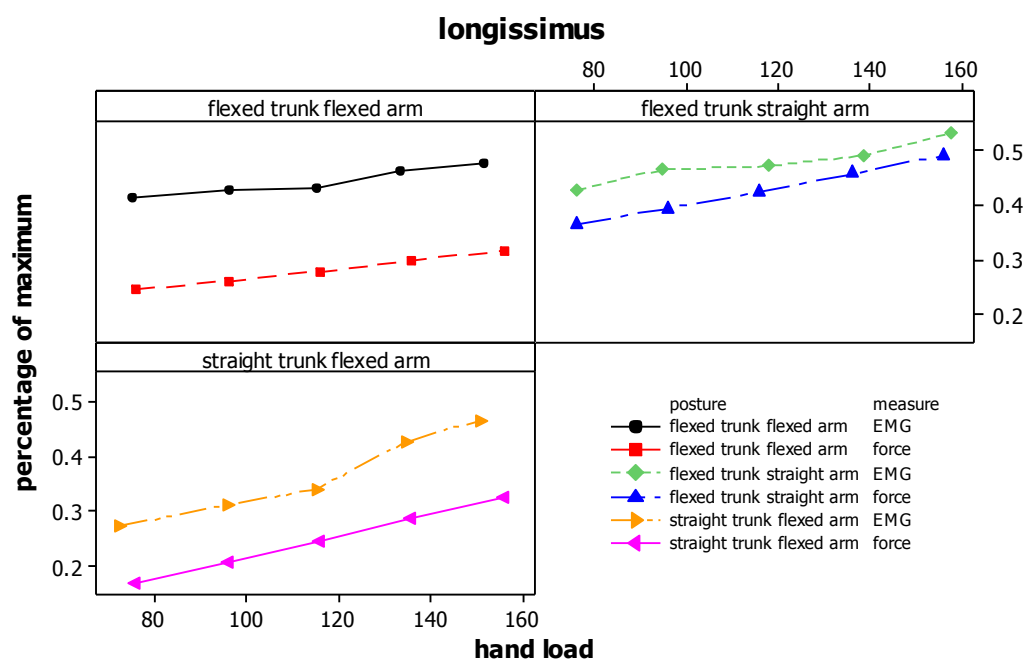


Figure 3.2 Percentage of maximum longissimus EMG RMS and predicted muscle force.

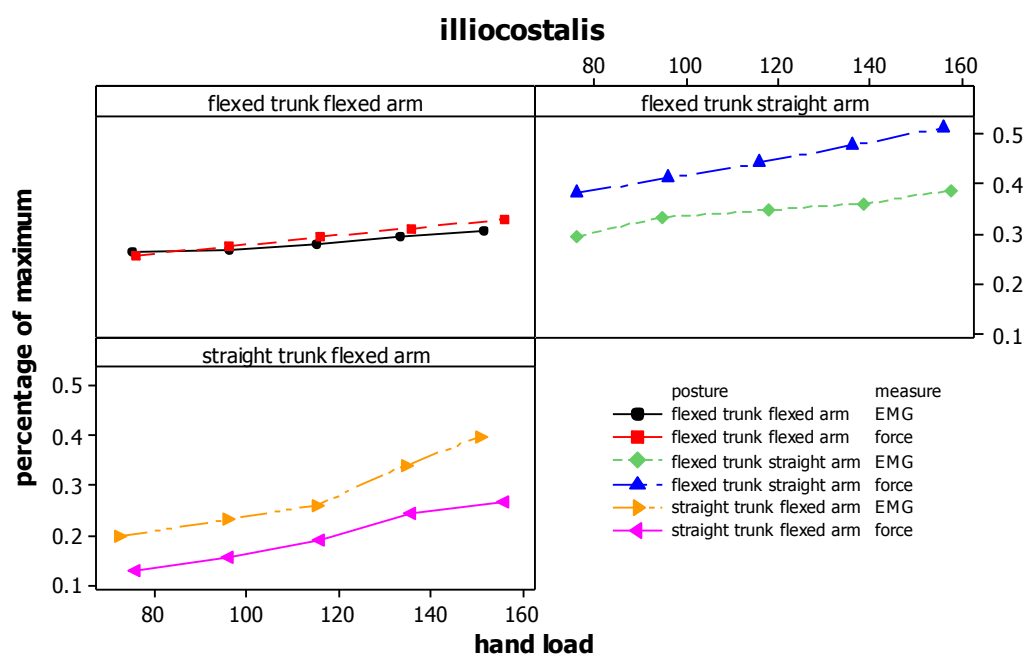


Figure 3.3 Percentage of maximum iliocostalis EMG RMS and predicted muscle force.

As expected, EMG and predicted forces of both muscles increased as hand loads increased in all three body postures. The increasing trend of EMG was somewhat variable but the predicted muscle forces varied almost linearly with hand load. The Pearson's correlation coefficients between EMG and predicted muscle forces reached 0.9800.

The percentage of maximum between EMG RMS and predicted muscle forces was not the same. In this study, the AnyBody Modeling System™ scaled the model linearly to fit 50 percentile European population according to the subject's weight and height, so the maximum muscle force defined in the AnyBody Modeling System™ may not be the same as that of the individual subject. To solve the problem, the AnyBody Modeling System™ provides a mechanism to scale the model more accurately according to some external force measurements, individual segment length and weight. Another way to get more accurate predicted results in comparison with the EMG is to test more subjects so as to cover the population. In that case, the scaling of the model based on mean and standard deviation of subjects' height and weight will be much more accurate, and the percentage of maximum force predicted on that will be closer to normalized EMG. In EMG assisted model [7, 14], they have also utilized certain gain factors to scale force based on normalized EMG for each muscle.

The joint compression and shear forces predicted by 3rd, 5th, and infinite order polynomial criteria in AnyBody™ with increasing hand loads were then determined and plotted in Figure 3.4 and Figure 3.5. For all three polynomial orders, as the hand load increased, the joint forces also increased. However, the joint force predicted by 3rd and

5th order increased abruptly when the hand load reached to maximum hand load 176N, which is not an expected physiological phenomenon. Rather than computational anomaly or singularity is a suspect for such abrupt fluctuation of joint compression force. To understand the reason behind this sudden fluctuation, the predicted individual muscle forces were further checked, and psoas major muscle was found to be suddenly activated when the hand load reached near 176N, and after that predicted joint forces and psoas major muscle force were somewhat converged. Personal communication with the main developer of AnyBody™ confirmed that activation of psoas major generate a great amount of force to lumbar joint [53]. The reason behind this problem may be that muscle with short moment arm in lumbar region may be predicted to suddenly generate great amount of force against external moment because the muscle with long moment arm is already saturated while using lower order criteria in high hand loads. This can be avoided when using infinite order criterion because muscles work more synergistically, and muscle with a short moment arm is activated all the time even the hand load is small. This problem is still under investigation, and it is possible that 3rd and 5th order criteria are not suitable for such a sophisticated whole body model investigation. The previous research by Arjmand and Shirazi-Adl [11] using 3rd order criterion was based a much simpler model.

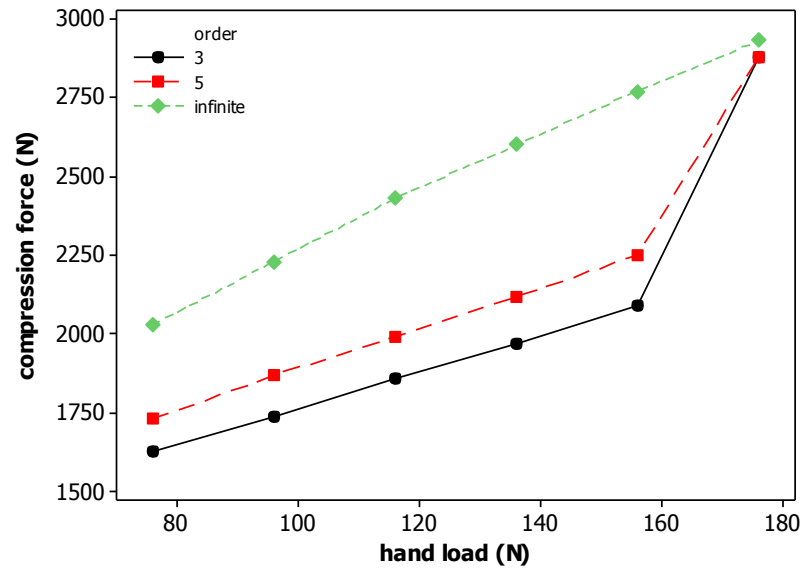


Figure 3.4 Predicted L4/L5 joint compression forces with gradually increasing hand load of the three criteria in flexed trunk straight arm posture.

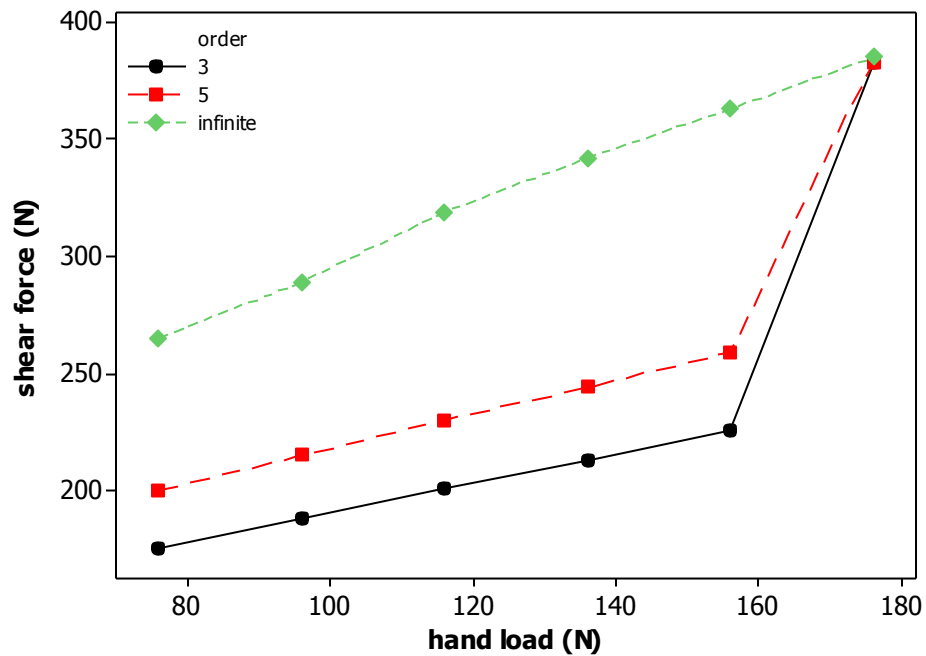


Figure 3.5 Predicted L4/L5 joint shear forces with gradually increasing hand load of the three criteria in flexed trunk straight arm posture.

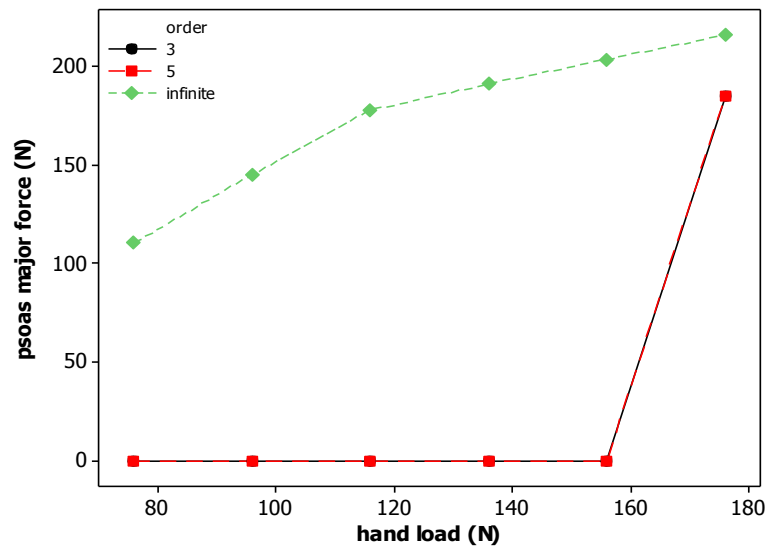


Figure 3.6 Predicted psoas major force with gradually increasing hand load of the three criteria in flexed trunk straight arm posture

Therefore, for lifting tasks simulated in AnyBody Modeling System™, infinite order polynomial (min/max) can predict muscle forces correlated with EMG well despite the scaling problem, and is more physiologically attractive in ergonomic investigation.

CHAPTER 4

ASYMMETRIC EFFECT IN DYNAMIC LIFTING TASK

This section describes the experimental study to investigate asymmetric effect in dynamic lifting task. Motion data in asymmetric lifting tasks was captured by a six-camera OptiTrack™ motion capture system, and then used to drive AnyBody™ model. Right erector spinae (RES), left erector spinae (LES), right external oblique (REO), left external oblique (LEO), right internal oblique (RIO) and left internal oblique (LIO) muscle forces were selected and investigated because they are important muscles in asymmetric lifting. L5/S1 joint forces were also selected to investigate LBD. The experimental details and results follow.

4.1 Methods and Materials

One healthy college student (1.73cm, 75kg) without any history of LBD during the past six months performed asymmetric lifting tasks of 0°, 30° and 60° with 30lb (13.6kg) dumbbell weights placed evenly in a plastic tray in OptiTrack™ Motion Capture Laboratory of Biomedical Engineering Department, New Jersey Institute of Technology. The lift origin was fixed at knuckle height (vertical height of 99.1 cm off the ground) and at a horizontal distance of approximately 53.3 cm from the center of the box to the spine. The experimental layout was dimensionally identical with Marras and Davis's study [18], so that the results could be compared. Asymmetric angles were taped on a force plate for feet positioning, including a sagittal symmetric position (0°), 30° and 60° to the right of the mid-sagittal plane. The force plate was used to collect ground reaction and moment data during the lifting. The force plate data was not used in this study, but will be used in later research to compare joint moments predicted by AnyBody™ with those derived

from force plate. By using a metal stand with a thin wooden board to place the plastic tray with dumbbell weights (Figure 4.1), marker blocking was minimized.

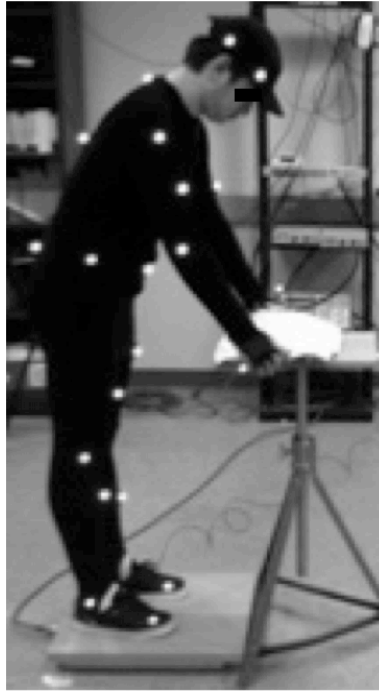


Figure 4.1 Asymmetric lifting task configuration.

Before the experiment, the participant was informed about the purpose and procedure of the experiment, and put on OptiTrack™ medium-size motion capture suit. With the help of laboratory assistant, thirty-four reflective markers were attached on the suit according to OptiTrack™ standard thirty-four-marker placement protocol [54]. After standard calibration and skeleton setting up procedure instructed by ARENA™ motion capture software [55], the motion data of lifting were collected through OptiTrack™ six-camera tripod setup [55] with 100 frames/seconds.

During the experiment, the participant performed three (asymmetric angles) lifting tasks, in a randomized order. The lifting task was first standing straight with feet

positioned along the tape at pre-defined angle, and then lifting from the fixed origin to upright position (holding the tray) without moving his feet.

4.2 Results

Raw mocap data of each marker was assigned to proper body positions to drive the skeleton in ARENA™ software. At certain instances, gaps in data may be caused by marker blocking, and gaps less than twenty frames were automatically filled by the algorithm in ARENA™. The data then was further smoothed with cut-off frequency of 6 Hz. Frames exported to “c3d” file were further chosen manually by checking vertical positions of left hand: beginning with the tray being lifted and ending with holding the tray still. After that, each marker positions were checked, and gaps more than twenty frames were filled manually by visual inspection. Figure 4.2 shows the initial frames of 0°, 30° and 60° asymmetric lifting simulated in inverse dynamic study by AnyBody™ model respectively.

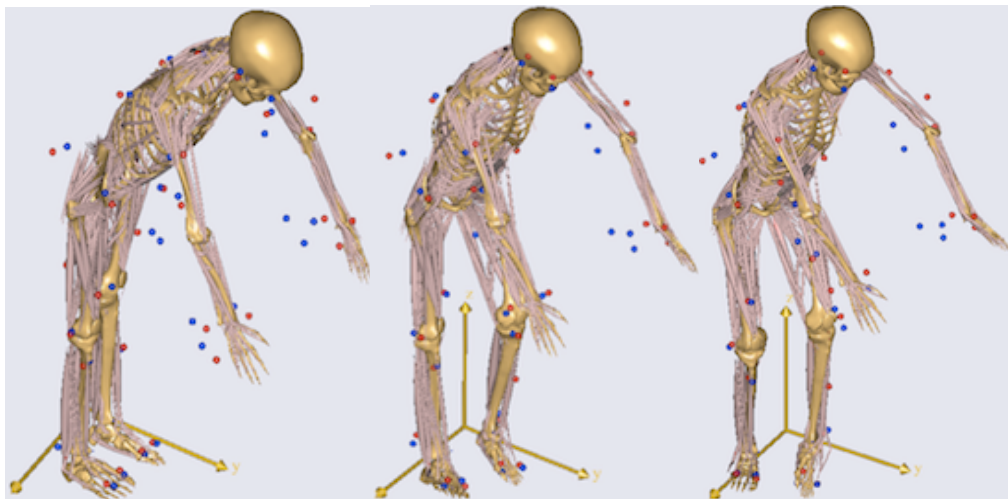


Figure 4.2 First frames of 0°, 30° and 60° asymmetric lifting initialized in inverse dynamic study by AnyBody™ model.

GaitLowerExtremityProject model in AMMRV1.31 was modified to suit the experimental task. Subsequently, each motion capture file was used to drive the AnyBody™ model. Approximately between 160 to 220 frames were generated by ARENA™ for individual trials. In biomechanical studies, customarily the mocap frame rate is reduced to save computational time. The default frame rate reduction value set in AnyBody™ software was 1/6th, and was used for further analysis. With the reduced set of frames, skeleton initial positioning, motion and parameter optimization, and inverse dynamic study routines were run within AnyBody™ software. On a Sony VAIO® E series laptop computer with 2.2 GHz dual-core CPU and 3GB RAM, each trial took approximately 2 hours of computation.

From the program output, maximum muscle forces of selected muscles are reported in Table 4.1. Only the muscle groups that developed more than 100 N force are reported. Rest of the muscle groups data were ignored for this study, since they will not have any real effect on back loading. The finding of muscle force are as following:

Table 4.1 Maximum Muscle Forces in Newton during Each Task

| | Asymmetric angle | | |
|------------------------------|------------------|------|------|
| | 0 | 30 | 60 |
| Right erector spinae (RES) | 1590 | 1360 | 1340 |
| Left erector spinae (LES) | 1370 | 1290 | 1310 |
| Right external oblique (REO) | 67 | 124 | 142 |
| Left external oblique (LEO) | 49 | 49 | 30 |
| Right internal oblique (RIO) | 234 | 179 | 150 |
| Left internal oblique (LIO) | 119 | 183 | 154 |

Followings are the main observations on muscle forces:

1. ES generated 1290N to 1590N forces, which was far exceeded the other muscles.
2. REO was 85.1% and 111.9% more active for 30° and 60° lifts compared to sagittal lift.

3. RIO exhibited complementary force activation, and was 23.5% and 35.9% less active for 30° and 60° lifts compared to sagittal lift.
4. LEO was insignificantly activated, and generated force less than 50N in the three asymmetric angles.
5. LIO was activated during the lifting tasks, but no significant difference noted between trials.

Erector spinae is the main extensor of trunk. When the erector spinae fascicles of one side act together, they produce combined lateral flexion and rotation to the same side [51]. During asymmetric lifts, the support of the external load is shifted from the large erector spinae muscles to smaller, less capable oblique muscles [20]. When lifting origin became more asymmetric toward right, trunk rotated and laterally flexed more toward right. Therefore, REO was more activated, and complementarily RIO was less activated. LEO played a minor role in right asymmetric lifting task, and the difference of activation for LIO may be due to variance of the motion. These observations were appropriate and were expected from the muscle mechanics and physiological point of view.

Maximum joint compressive and shear forces at L5/S1 joint are presented in Table 4.2. L5/L1 maximum compression force reduced 14.1% and 15.4% for 30° and 60° respectively comparing with 0°; A/P shear force reduced 16.3% and 22.5% for 30° and 60° respectively comparing with 0°; lateral shear force reduced 26.4% and increased 10.5% for 30° and 60° respectively comparing with 0°. In general, joint forces reduced as lifting origin became more asymmetric.

Table 4.2 Maximum Joint Forces in Newton during Each Task

| | Asymmetric angle | | |
|--------------------|------------------|------|------|
| | 0 | 30 | 60 |
| L5S1 compression | 3690 | 3170 | 3120 |
| L5S1 A/P shear | 675 | 565 | 523 |
| L5S1 lateral shear | 28 | 20 | 31 |

Biomechanically, ES has smaller moment arm than oblique muscles referring to lumbar joint, so ES is less efficient in supporting external moment generated by upper body weight and hand loads. When the support of the external moment shifts from ES to oblique muscles, which also means shifting to more efficient muscles, the joint forces should be reduced. However, oblique muscles are much weaker than ES, so they are less activated during symmetric lifting to minimize muscle fatigue. Furthermore, from observation (Figure 4.2), the participant tended to squat more as lifting origin became more asymmetric, which may also be a strategy of our body to reduce joint forces.

According to NIOSH [56], the tolerance level for compression loading of the spine is expected to be around 3400 N. At this level of compression, micro fractures of the vertebral endplate begin to occur. The threshold limits for spine lateral and A-P shear are not as well documented, but they are probably less than 900 N. Reducing A-P shear and compressive forces should be considered a priority to prevent LBD [18]. In this study, joint forces did not exceed limitation except compression force during symmetric lifting. However, if certain factors such as lifting speed, lifting height and lifting weight become more demanding, joint forces may exceed the tolerance level, and workers working for years under those circumstances may develop LBD.

The average maximum L5/S1 compression force derived from ten subjects by Marras et al.'s EMG assisted model [18] was approximately 3600N, 3900N and 4050N for asymmetric lifting of 0°, 30° and 60° toward right. The forces increased as the lifting origin became more asymmetric, but the compression force in sagittal lifting matched well with this study. A-P shear force was approximately 910N, 850N and 830N for 0°, 30° and 60° asymmetry respectively. Comparing with this study, both A-P compression

force decreased as the lifting origin became more asymmetric, but the force predicted by Marras et al. was about 235N to 285N higher than this study. Lateral shear force predicted by them ranged from 210N to 350N, which was far higher than the values predicted by AnyBody™ in this study. Generally, they found compression and lateral shear forces increased as the lift origin became more asymmetric, whereas A-P shear force decreased, and muscles on the opposite side of the body referring to lifting asymmetric direction were activated more than muscles on the same side. However, as mentioned in sub-section 2.2.6, using EMG in dynamic lifting is problematic. Their results were based on averages of ten subjects, but the standard deviations were quite high. Therefore, although their model may consider muscle co-contraction better, which predicted joint forces higher than this study, their results may not be conclusive.

CHAPTER 5

CONCLUSION AND FUTURE WORK

This study provides up-to-date literature review on current biomechanical models for lifting tasks. All these models incorporate simplifying assumptions that should be taken into consideration when one applies these models to investigate lower back stress. The AnyBody Modeling System™ provides most detailed anatomical model, but the optimization criteria to predict muscle recruitment for lifting tasks were not completely validated.

An isometric pulling experiment was conducted to study the correlation between muscle activity measured by EMG and predicted muscle forces from AnyBody™ with increasing hand loads. With infinite order polynomial predicted percentage of maximum muscle forces achieved 98% correlation with normalized EMG RMS. Considering predicted joint forces, infinite order polynomial criterion, performed better than 3rd and 5th order polynomials. Motion data during lifting tasks of 0°, 30° and 60° asymmetry toward right with 30lb (13.6kg) weight was then collected by OptiTrack™ six-camera mocap system to drive AnyBody™ model, and asymmetric effect was investigated. ES was the most activated muscle during both symmetric and asymmetric lifting tasks. When lifting origin became more asymmetric toward right, REO was more activated, and complementarily RIO was less activated. LEO played a minor role in right asymmetric lifting task, and the difference of activation for LIO may be due to variance of the motion. Because oblique muscles with larger moment arms can support external moment more efficiently, and subject tended to squat more as lifting origin became more asymmetric, L5/S1 joint forces decreased during more asymmetric lifting.

Based on this thesis, further work is expected as following:

1. The optimization criteria should be further investigated and modified with muscle co-contraction being considered, so as to get more accurate results.
2. When biomechanical modeling was utilized, care should be taken on the scaling issue of the model. Data captured through force plate can be utilized in future to investigate the necessary scaling of the outputs.
3. Even in biomechanical modeling and simulating investigation, more subjects should be used to increase the repeatability.
4. Others factors such as lifting height and lifting speed should be investigated by AnyBody™ model.

REFERENCE

- [1] Z. Cheung, *et al.*, "DHHS (NIOSH) Publication No. 2007-13: Ergonomic Guidelines for Manual Material Handling," ed, April 2007.
- [2] Bureau of Labor Statistics, "Nonfatal occupational injuries and illnesses requiring days away from work, 2009," ed, 2010.
- [3] Eastman Kodak Company Co., Human Factor Section, *Ergonomic Design for People at Work*, 2nd ed. vol. 2. New York, NY: Van Nostrand Reinhold 1986.
- [4] L. Manchikanti, *et al.*, "Comprehensive review of epidemiology, scope, and impact of spinal pain," *Pain Physician*, vol. 12, 2009.
- [5] N. Arjmand and A. Shirazi-Adl, "Model and in vivo studies on human trunk load partitioning and stability in isometric forward flexions," *Journal of Biomechanics*, vol. 39, pp. 510-521, 2006.
- [6] M. de Zee, *et al.*, "A generic detailed rigid-body lumbar spine model," *Journal of Biomechanics*, vol. 40, pp. 1219-1227, 2007.
- [7] S. M. McGill and R. W. Norman, "1986 Volvo award in biomechanics: Partitioning of the L4-L5 dynamic moment into disc, ligamentous, and muscular components during lifting," *Spine*, vol. 11, pp. 666-678, 1986.
- [8] M. A. Nussbaum and D. B. Chaffin, "Development and evaluation of a scalable and deformable geometric model of the human torso," *Clinical Biomechanics*, vol. 11, pp. 25-34, 1996.
- [9] A. B. Schultz and G. B. J. Anderson, "Analysis of loads on the lumbar spine," *Spine*, pp. 76-82, 1981.
- [10] J. C. Bean, *et al.*, "Biomechanical model calculation of muscle contraction forces: A double linear programming method," *Journal of Biomechanics*, vol. 21, pp. 59-66, 1988.
- [11] N. Arjmand and A. Shirazi-Adl, "Sensitivity of kinematics-based model predictions to optimization criteria in static lifting tasks," *Medical Engineering and Physics*, vol. 28, pp. 504-514, 2006.
- [12] J. Rasmussen, *et al.*, "Muscle recruitment by the min/max criterion - A comparative numerical study," *Journal of Biomechanics*, vol. 34, pp. 409-415, 2001.
- [13] M. K. Chung, *et al.*, "A novel optimization model for predicting trunk muscle forces during asymmetric lifting tasks," *International Journal of Industrial Ergonomics*, vol. 23, pp. 41-50, 1998.
- [14] W. S. Marras and K. P. Granata, "The development of an EMG-assisted model to assess spine loading during whole-body free-dynamic lifting," *Journal of Electromyography and Kinesiology*, vol. 7, pp. 259-268, 1997.

- [15] NIOSH, "DHHS (NIOSH) Publication No. 91-100: Selected Topics in Surface Electromyography for Use in the Occupational Setting: Expert Perspective," ed, 1992.
- [16] S. A. Ferguson, *et al.*, "Quantification of back motion during asymmetric lifting," *Ergonomics*, vol. 35, pp. 845-859, 1992.
- [17] W. G. Allread, *et al.*, "Trunk kinematics of one-handed lifting, and the effects of asymmetry and load weight," *Ergonomics*, vol. 39, pp. 322-334, 1996.
- [18] W. S. Marras and K. G. Davis, "Spine loading during asymmetric lifting using one versus two hands," *Ergonomics*, vol. 41, pp. 817-834, 1998.
- [19] Y. Hattori, *et al.*, "Effects of box weight, vertical location and symmetry on lifting capacities and ratings on category scale in Japanese female workers," *Ergonomics*, vol. 43, pp. 2031-2042, 2000.
- [20] W. S. Marras and G. A. Mirka, "A comprehensive evaluation of trunk response to asymmetric trunk motion," *Spine*, vol. 17, pp. 318-326, 1992.
- [21] AnyBody Technology A/S. (2011, 4/20). *AnyBody Technology A/S*. Available: <http://www.anybodytech.com/>
- [22] AnyBody Technology A/S. (10/13/2010). *The AnyBody Modeling System™*. Available: <http://www.anybodytech.com/index.php?id=26>
- [23] M. Grujicic, *et al.*, "Musculoskeletal computational analysis of the influence of car-seat design/adjustments on long-distance driving fatigue," *International Journal of Industrial Ergonomics*, vol. 40, pp. 345-355, 2010.
- [24] AnyBody Technology. (05/02/2010). *AnyBody™ Tutorials (Version 4.2.0 ed.)*.
- [25] J. Z. Wu, *et al.*, "Modeling the finger joint moments in a hand at the maximal isometric grip: The effects of friction," *Medical Engineering and Physics*, vol. 31, pp. 1214-1218, 2009.
- [26] J. Z. Wu, *et al.*, "Analysis of musculoskeletal loadings in lower limbs during stilts walking in occupational activity," *Annals of Biomedical Engineering*, vol. 37, pp. 1177-1189, 2009.
- [27] J. Z. Wu, *et al.*, "Analysis of musculoskeletal loading in an index finger during tapping," *Journal of Biomechanics*, vol. 41, pp. 668-676, 2008.
- [28] A. Freivalds, *et al.*, "A dynamic biomechanical evaluation of lifting maximum acceptable loads," *Journal of Biomechanics*, vol. 17, pp. 251-262, 1984.
- [29] D. B. Chaffin, *et al.*, *Occupational Biomechanics*, 4th Edition ed.: J. Wiley & Sons, Inc., 2006.
- [30] K. H. Kim, *et al.*, "Modelling of shoulder and torso perception of effort in manual transfer tasks," *Ergonomics*, vol. 47, pp. 927-944, 2004.
- [31] A. Schultz, *et al.*, "Loads on the lumbar spine. Validation of a biomechanical analysis by measurements of intradiscal pressures and myoelectric signals," *Journal of Bone and Joint Surgery - Series A*, vol. 64, pp. 713-720, 1982.

- [32] University of Michigan. (4/20/2011). *3D Static Strength Prediction Program™*. Available: <http://www.engin.umich.edu/dept/ioe/3DSSPP/>
- [33] N. Arjmand, *et al.*, "Wrapping of trunk thoracic extensor muscles influences muscle forces and spinal loads in lifting tasks," *Clinical Biomechanics*, vol. 21, pp. 668-675, 2006.
- [34] N. Arjmand, *et al.*, "Trunk biomechanical models based on equilibrium at a single-level violate equilibrium at other levels," *European Spine Journal*, vol. 16, pp. 701-709, 2007.
- [35] N. Arjmand, *et al.*, "Comparison of trunk muscle forces and spinal loads estimated by two biomechanical models," *Clinical Biomechanics*, vol. 24, pp. 533-541, 2009.
- [36] N. Arjmand, *et al.*, "A comparative study of two trunk biomechanical models under symmetric and asymmetric loadings," *Journal of Biomechanics*, vol. 43, pp. 485-491, 2010.
- [37] N. Arjmand, *et al.*, "Predictive equations to estimate spinal loads in symmetric lifting tasks," *Journal of Biomechanics*, vol. 44, pp. 84-91, 2011.
- [38] N. Bogduk, "A reappraisal of the anatomy of the human lumbar erector spinae," *Journal of Anatomy*, vol. 131, pp. 525-540, 1980.
- [39] S. M. McGill and R. W. Norman, "Effects of an anatomically detailed erector spinae model on L4/L5 disc compression and shear," *Journal of Biomechanics*, vol. 20, pp. 591-600, 1987.
- [40] Center for Ergonomics, the University of Michigan. (June 2010). *3D Static Strength Prediction Program™ Version 6.0.4 User's Manual*. Available: http://www.engin.umich.edu/dept/ioe/3DSSPP/Manual_604.pdf
- [41] J. Cholewicki, *et al.*, "Comparison of muscle forces and joint load from an optimization and EMG assisted lumbar spine model: Towards development of a hybrid approach," *Journal of Biomechanics*, vol. 28, pp. 321-331, 1995.
- [42] S. M. McGill, *et al.*, "A simple polynomial that predicts low-back compression during complex 3-D tasks," *Ergonomics*, vol. 39, pp. 1107-1118, 1996.
- [43] H. J. Wilke, *et al.*, "Intradiscal pressure together with anthropometric data - A data set for the validation of models," *Clinical Biomechanics*, vol. 16, 2001.
- [44] D. Kee and M. K. Chung, "Comparison of prediction models for the compression force on the lumbosacral disc," *Ergonomics*, vol. 39, pp. 1419-1429, 1996.
- [45] S. L. Fischer, *et al.*, "Methodological considerations for the calculation of cumulative compression exposure of the lumbar spine: A sensitivity analysis on joint model and time standardization approaches," *Ergonomics*, vol. 50, pp. 1365-1376, 2007.
- [46] W. S. Marras, "Industrial electromyography (EMG)," *International Journal of Industrial Ergonomics*, vol. 6, pp. 89-93, 1990.

- [47] L. Hansen, *et al.*, "Anatomy and Biomechanics of the Back Muscles in the Lumbar Spine With Reference to Biomechanical Modeling," *Spine*, vol. 31, pp. 1888-1899, August 1, 2006 2006.
- [48] AnyBody Technology A/S. (2010, Mar 12th). *Lumbar spine model-spine rhythm presentation*. Available: <http://wiki.anyscript.org/images/b/b6/Spinerhythm.pdf>
- [49] AnyBody Technology A/S. (2010, Mar 12th). *Lumbar spine model-intra abdominal pressure* Available: http://wiki.anyscript.org/index.php/AnyBody_Managed_Model_Repository:_Body_Models#Lumbar_spine
- [50] H. J. Wilke, *et al.*, "New in vivo measurements of pressures in the intervertebral disc in daily life," *Spine*, vol. 24, pp. 755-762, 1999.
- [51] N. Palastanga, *et al.*, *Anatomy and Human Movement*, 4th ed., 2002.
- [52] R. J. Parkinson, *et al.*, "A comparison of low back kinetic estimates obtained through posture matching, rigid link modeling and an EMG-assisted model," *Applied Ergonomics*.
- [53] AnyBody Technology A/S. (2011, 4/29). *AnyScript Community™* Available: <http://forum.anyscript.org/showthread.php?p=13195#post13195>
- [54] NaturalPoint® Inc. (2011, 4/20). *Arena/Expression Marker Placement Guide*. Available: <http://www.naturalpoint.com/optitrack/support/manuals/arena/>
- [55] NaturalPoint® Inc. (2011, 4/20). *ARENA™ Tutorial Videos*. Available: <http://www.naturalpoint.com/optitrack/products/motion-capture/tutorials/arena/>
- [56] NIOSH, "Work practices guide for manual lifting, NIOSH Technical Report No. 81-122," ed, 1981.